

Height Distribution of Refractivity Structure Constant from Radiosonde Observations

P K PASRICHA, MAHENDRA MOHAN, D K TIWARI & B M REDDY
Radio Science Division, National Physical Laboratory, New Delhi 110012

Received 22 April 1982

Radio refractivity structure constant C_n^2 and its height distribution under varied meteorological conditions are evaluated from routine radiosonde observations. The mixing length theory in conjunction with Tatarskii's theoretical formulation permits C_n^2 evaluation from mean meteorological fields. The C_n^2 values so deduced are normalized to the existing turbulence conditions, obtained through an empirical relationship between thermal atmospheric stability and a parameter that characterizes turbulence.

1 Introduction

The scattered power in a tropospheric-scatter system depends on the spatial distribution of radio refractive index fluctuations in the turbulent atmosphere. The spectral distribution of refractivity fluctuations $\Phi(K)$ is characterized by two parameters, viz. the spectral intensity in terms of Tatarskii's structure constant C_n^2 and the spectral slope m in the high frequency region of the spectrum. The latter determines the size of the turbulent eddies in the scattering medium. The tropospheric-scatter experiments usually make use of spectral wave number of eddies in the inertial subrange of the turbulence spectrum. The effective size of the eddies responsible for the scattering is given by the first Fresnel zone at the receiver, i.e. $(\lambda L)^{1/2}$, λ being the observing wavelength and L the radio path length. Tropospheric radio wave propagation in the S-band and at higher frequencies with path length $L \sim 100$ km, and an outer scale of turbulence characteristic of the inertial subrange $L_0 \approx 100$ m, yields $(\lambda L)^{1/2} < L_0$. At UHF and lower frequencies¹, however, $(\lambda L)^{1/2} \approx L_0$. A typical estimate of C_n^2 lies in the range 10^{-14} to 10^{-15} corresponding to a height interval of 1 to 2 km (Refs. 2-5). In the literature, C_n^2 values have not been quoted in relation to the m values of the corresponding turbulence spectrum under varied meteorological conditions.

Under certain assumptions, model height profiles of C_n^2 have been computed using the routine radiosonde (mean) profiles of temperature, humidity and wind. Gossard⁶ makes use of the basic definition of structure constant in conjunction with the mixing length concept⁷ to compute (up to 4 km) C_n^2 for different air mass types. Such (large) C_n^2 values appropriate to a scale greater than L_0 are normalized to turbulence's scale by making use of a model of the height variation

of optical refractivity structure put forth by Hufnagel⁸. The height distribution of C_n^2 so computed is compared with the ones deduced from the data obtained with the Millstone Hill radar observations. VanZandt *et al.*⁹ have attempted model computations of C_n^2 (in the range 4 to 16 km) from a theoretical formulation valid under conditions of homogeneous and isotropic turbulence introduced by Tatarskii¹⁰. L_0 occurs in the formulation of C_n^2 explicitly and is taken to be ≈ 10 m. With other parameters (to be described in Section 2) having values appropriate to turbulence conditions, the refractivity gradient at the different radiosonde levels is appropriate to mean meteorological parameters. The efforts in this model computations have been toward estimation of a fraction of the scattering volume that is turbulent. Model C_n^2 values are found to be in reasonable agreement with the VHF Doppler radar measurements that are averaged over the scattering volume and over 1 hr in time.

This paper presents model calculations of C_n^2 and its height distribution from mean meteorological parameters by combining the earlier two approaches. The concept of mixing length enables various eddy diffusion coefficients to be computed from mean profile gradients at the radiosonde levels. A scale of turbulence of the order of mixing length (and regarded equal to L_0) along with the computed coefficients permits C_n^2 evaluation from the theoretical formulation of Tatarskii. The empirical relationship of Gjessing *et al.*¹¹ between the atmospheric stability (in terms of Väisälä-Brunt frequency) and spectral slope (a parameter that characterizes turbulence) is invoked to obtain distribution of C_n^2 for turbulence conditions at three 'significant' radiosonde levels. The values so computed are compared with the model calculations of Gossard⁶.

2 Methodology of Structure Constant Evaluation

The turbulence structure constant for the radio refractivity under conditions of homogeneous and isotropic turbulence is given by^{9,10}

$$C_n^2 = a_1^2 \alpha' L_0^{4/3} M^2 \quad \dots(1)$$

$a_1^2 \equiv Fa^2$, a^2 being the universal constant, α' a ratio of coefficients of eddy conductivity and eddy viscosity, L_0 outer scale of turbulence, M the vertical gradient of refractivity, and F signifies fraction of the region that is turbulent. M is given by

$$M = -\frac{77.6 \times 10^{-6}}{T^2} p \left(1 + \frac{15500q}{T} \right) \times \left[\frac{dT}{dz} + r_a - \left(\frac{7800}{1 + (15500q/T)} \frac{dq}{dz} \right) \right] \quad \dots(2)$$

p being the atmospheric pressure, T the absolute temperature, q the specific humidity (\approx mixing ratio e) and γ_a the adiabatic lapse rate. In the present approach, L_0 is regarded to be of the order of mixing length.

The mixing length is obtained explicitly from the vertical turbulent diffusion of water vapour, represented in the form

$$\rho_v(Z) = \rho_v(Z_0) \exp \int_{Z_0}^Z \left(-\frac{1}{\zeta_v} - \frac{1}{H} \right) dZ \quad \dots(3)$$

$\rho_v(Z_0)$ being the water vapour density at the reference level, $\rho_v(Z)$ the density at the subsequent radiosonde levels, H the scale height of the dry air, and ζ_v the mixing length in the case of eddy diffusion of water vapour. This mixing length is regarded to be approximately equal to (strictly greater than) the mixing length in the case of eddy diffusion of momentum. With the coefficient of eddy diffusivity defined by $K_v = W\zeta_v$, the vertical eddy flux of water vapour is given by

$$F_v = -\rho K_v \frac{dq}{dz} \quad \dots(4)$$

ρ being the density of air and W the mean wind speed. Water vapour distribution significantly determines the vertical eddy flux of sensible heat in air. The effect is brought about through the dependence of the specific heat of air on specific humidity, and through water vapour adding to air density and buoyancy¹². In a nearly dry atmosphere (conditions normally prevailing above ~ 1 km), the moisture gradient determines the sensible heat flux¹³, and the coefficient of eddy conductivity K_H may be described in terms of the eddy flux of the water vapour as

$$K_H = \left[\frac{1}{\rho C_p \left(\frac{dT}{dz} \right)} \right] L_v F_v \quad \dots(5)$$

L_v being the latent heat of evaporation and C_p the specific heat at constant pressure. The coefficient of eddy viscosity (momentum) K_M is defined in terms of outer scale of turbulence as,

$$K_M = L_0^2 \left| \frac{dw}{dz} \right| \quad \dots(6)$$

α' in Eq. (1) is then given by the ratio K_H/K_M .

For turbulence conditions, the parameters a^2 and α' may be taken to be 2.8 (Ref. 14) and 1 respectively. The constant a_1^2 , as introduced in Eq. (1), to be inferred from mean meteorological parameters, is expected to be less than 1 (Ref. 10). The constant a_1^2 in the present approach is the normalization factor to convert C_n^2 values, obtained from Eq. (1) with mean meteorological parameters, to turbulence conditions. The estimation of C_n^2 for turbulence conditions associated with a given spatial averaging (and therefore static stability) must invoke additional assumptions. A straightforward approach is to look for an empirical relationship between static stability and a parameter that characterises turbulence. Gjessing *et al.*¹¹ have developed an empirical correlation between Väisälä-Brunt frequency v^2 (a measure of thermal atmospheric stability) and the slope of the refractivity spectrum. The beam-swinging scatter experiment measures the average value of the slope of the refractivity spectrum $\Phi(K)$ in the height interval 2 to 11 km. The atmospheric stability parameter v^2 is obtained from the simultaneous radiosonde sounding observations given by

$$v^2 = \frac{g}{T} \left(\frac{dT}{dz} + 0.055 T_I + \frac{g}{c_p} \right) \quad \dots(7)$$

dT/dz being the temperature gradient per kilometre, g the acceleration due to gravity; T and dT/dz are the average values over 1 to 2 km height interval for the significant level '1', 2 to 3 km for level '2' and 3 to 4.5 km for level '3'; T_I is the initial temperature of each of the three significant levels. Actually, v^2 should have been averaged over the entire height range. The parameter v^2 was computed for three significant levels to ascertain the validity of Eq. (7) for height interval less than the prescribed one in the original formula. An approximately equal value of v^2 obtained at three levels approves the sub-division of the height interval at the significant levels. Therefore, the characteristics of turbulence at the three significant levels shall remain the same in the present approach. The spectral slope m corresponding to a v^2 value is given by the empirical relation

$$m = -40.6 + 7.08 v^2 \quad \dots(8)$$

From the set of data points presented by Gjessing *et al.*¹¹ m varies from $-5/3$ to $-22/3$ corresponding to dT/dz variation from -8 to -5°C km^{-1} . The lower

value of lapse rate may well set the limit for turbulence occurrence. The high spectrum slope values are likely to be due to the presence of thin stratified layers in the medium. The parameter C_n^2 associated with layered structures is expected to be of greater magnitude compared to that of turbulent eddies. This is due to the coherent nature of scattering (partial reflection) from stratified layers compared to incoherent scattering in the other situation. For turbulence conditions, from the little experimental data on C_n^2 , no one-to-one correspondence of C_n^2 and m is found. In the absence of such a relationship, a C_n^2 value of $5 \times 10^{-15} m^{-2.3}$ at 1.5 km is taken to compute the normalizing constant a_1^2 , irrespective of the spectral slope value. It may be noted that C_n^2 so deduced for a $|m|$ value greater than 11/3 (the Kolmogorov's spectral slope) may reflect the presence of stratified structures such that the computed C_n^2 value is more than the actual value.

3 Model Calculation of Structure Constant

Model structure constant calculations have been carried out, using the monthly mean fields of temperature, humidity and wind at 0530 and 1730 hrs LT, for various seasons, for the coastal station Trivandrum.

For the computations presented in this paper, in the lower troposphere (upto ~ 4.5 km), humidity and (indirectly) wind speed predominantly contribute to structure constant. The smoothed height profiles of mixing ratio of water vapour for the seasons, viz. premonsoon, monsoon, post-monsoon and winter, are presented in Fig. 1. The actually observed resultant mean wind speed profiles for the corresponding seasons are also depicted in Fig. 1. The mixing ratio for the post-monsoon is higher compared to premonsoon,

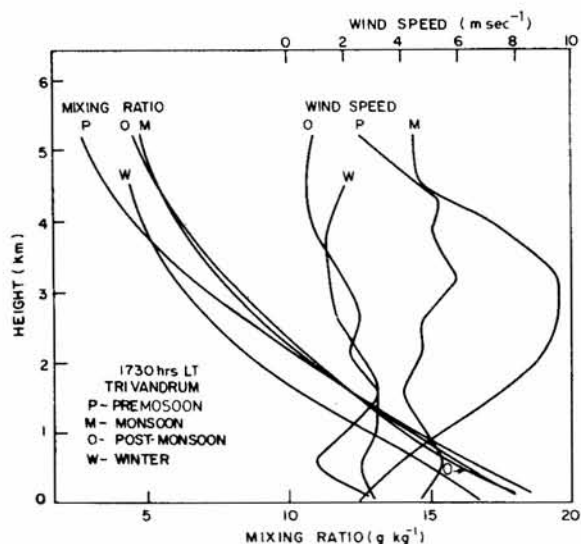


Fig. 1—Smoothed vertical profiles of mixing ratio of water vapour at 1730 hrs LT

but reverse is the case for mean wind speed. Thus, the eddy water vapour flux is higher for the premonsoon compared to post-monsoon. The apparently insignificant differences in slopes of the mixing ratio distributions, in fact, lead to substantial differences in mixing length distributions obtained from relation (3). In Eq. (3), the scale height of air is taken to be 6.5 km. The reference level is the radiosonde level corresponding to a barometric pressure of 1000 mbar. The vertical profiles of mixing length so deduced are presented in Fig. 2. The profiles of coefficient of eddy conductivity computed using the profiles of mixing length and wind speed are also shown in Fig. 2. In winter, a decrease in the mixing length, overwhelmed by a decrease in the temperature gradient, results in a sharp increase in the coefficient of eddy conductivity. At a given height, the mixing length is the largest for the monsoon season and the least for the winter season; the post-monsoon mixing length being greater than the premonsoon one. The mixing length is a measure of the efficiency of the turbulent diffusion; it increases with increased mixing length. The enhanced turbulent diffusion for the monsoon, aided by large wind gradient, results in profound mixing of the atmospheric medium. In general, turbulent diffusion decreases with increasing distance from the surface of the earth. Though eddy diffusion of water vapour is slower than the eddy diffusion of momentum, the (large) mixing length for water vapour, obtained from Eq. (3), is regarded to represent eddy diffusion of momentum. The coefficient of eddy viscosity depends on the mixing length and the vertical shear of mean wind speed [relation (6)]. The coefficient of eddy conductivity, on the other hand, depends on the mean wind speed [relation (5)]. Thus the coefficient of eddy conductivity is higher in the premonsoon than in the post-monsoon season. This is to be compared with the fact that the temperature gradient at different radiosonde levels is higher in the premonsoon than in the post-monsoon season. The apparent increase of coefficient of conductivity with height, for the winter season, in Fig. 2, is due to a sharp fall in eddy diffusion with height. It may be pointed out that the temperature gradient is the

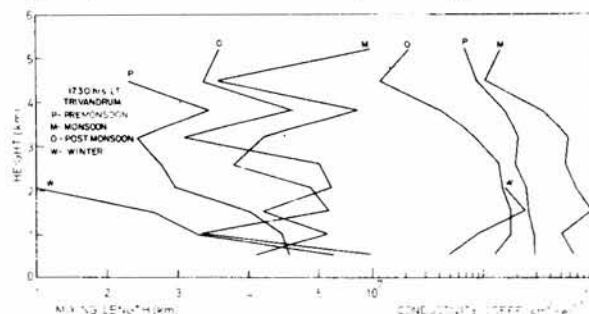


Fig. 2—Vertical profiles of mixing length corresponding to the mixing ratio profiles of Fig. 1.

Table 1—Model Structure Constant Calculations with $a_1^2 = 10^{-4}$ for Trivandrum

Season	Level	0530 hrs LT			1730 hrs LT			A model C_n^2 variation of Gossard ⁶
		α'	C_n^2 ($m^{-2.3}$) ($\times 10^{-15}$)	m ($\times 3$)	α'	C_n^2 ($m^{-2.3}$) ($\times 10^{-15}$)	m ($\times 3$)	
Premonsoon	1	1.2	7	-16	0.9	4	-15	Level 1: 5×10^{-15}
	2	0.7	2	-15	2.3	4	-13	
	3	0.6	0.4	-15	2.6	2	-15	
Monsoon	1	0.8	6	-15	1.5	5	-13	Level 2: 3×10^{-15}
	2	1.5	5	-19	2.5	6	-17	
	3	0.3	2	-17	0.7	3	-15	
Post-monsoon	1	0.6	3	-14	1.0	3	-14	Level 3: 1×10^{-15}
	2	U	U	U	0.7	2	-15	
	3	U	U	U	0.2	0.2	-18	
Winter	1	0.7	3	-16	0.3	1	-9	
	2	U	U	U	U	U	U	
	3	U	U	U	U	U	U	

Level 1: 1-1.5 km U: Unresolved
 2: 2.5-3 km
 3: 4-4.5 km

highest in the winter. Due to enhanced turbulent diffusion in the monsoon, the conductivity is the greatest. This is contrary to the fact that the temperature gradient is higher in the premonsoon than in the monsoon. The coefficient α' in Eq. (1) is the ratio K_H/K_M . The values of α' , at the two local times, and in different seasons are given in Table 1. The C_n^2 computations carried out, using Eq. (1), with $a_1^2 = 10^{-4}$ are presented in Table 1. The reasons for choosing a value of a_1^2 as 10^{-4} are described below. The spectral slope values at significant levels obtained from relations (7) and (8) are also presented in Table 1. As visualized from Table 1, the spectral slope at various significant levels does not show marked variation. This suggests that turbulence associated with different significant levels retains roughly the same characteristics. The spectral slope in the nighttime is greater than in the daytime, since nighttime is marked by stratified layered structures compared to turbulent eddies in the daytime. The spectral slope for the nighttime-first significant level is not large enough, since the averaging height interval in Eqs (7) and (8) extends from 1 km and not from ground. Further, the spectral slope is higher in the monsoon and post-monsoon than in the premonsoon season or winter. The reason is that the temperature gradient in the former seasons are less than in the latter ones. Thus increase in spectral slope may be correlated with extended stability of the atmospheric medium, as presented empirically by Gjessing *et al.* In the absence of a systematic relationship between C_n^2 and spectral slope, the normalization of the computed C_n^2 is performed with a typical turbulence $-C_n^2$ value of $5 \times 10^{-15} m^{-2.3}$ at a height of 1.5 km leading to $a_1^2 \approx 10^{-4}$.

4 Discussion

The decrease of C_n^2 with height is evident in Table 1. The decrease is, however, more pronounced at the level of 4-4.5 km. The model calculations of Gossard⁶ show large variation of C_n^2 about its mean value in a given air mass as well as variation from one air mass type to another. A rather systematic decrease of C_n^2 taken from these calculations is included in Table 1. A large scatter of C_n^2 from tropospheric scatter observations at a height of 1.5 km lies in the range of 1.4×10^{-13} to $4.4 \times 10^{-16} m^{-2.3}$ (Ref. 15). Vertical profile of C_n^2 with the Poker Flat phased array radar in Alaska shows a decrease of C_n^2 by an order of magnitude in the height interval of 2.5 to 4.5 km. In Table 1, C_n^2 is higher, at the first significant level, in the nighttime than in the daytime. At higher levels, however, C_n^2 is higher in the daytime compared to nighttime value. This is to be expected, since nighttime turbulence is marked by layered structures and C_n^2 associated with such strata is higher than that associated with turbulent eddies¹⁶. A higher C_n^2 value at the first significant level in the nighttime compared to daytime is consistent with the statistics of C_n^2 , obtained over a period of 1 yr in Colorado at a height of 805 m (Ref. 4). From the limited data analyzed for a single coastal station, the height variation of C_n^2 is more pronounced in the premonsoon, post-monsoon and winter, in that order. The decrease is particularly enhanced at nighttime. This aspect brings out the limitations of the methodology adopted in this paper. The mixing ratio profiles cannot be resolved for the scale height computations (marked U-Unresolved in Table 1) at higher levels corresponding to C_n^2 values of $\lesssim 10^{-16} m^{-2.3}$, a typical value at a height of 5 km. The

decrease of C_n^2 in the monsoon is not rapid, since turbulent diffusion is maintained at a steady magnitude throughout the height interval.

In the methodology adopted in this paper, the choice of a_1^2 is rather oversimplified. The dependence of a_1^2 on turbulence conditions (which vary from station to station) may be visualized through its dependence on the size of eddies characteristic of turbulence. The wavelength of observations determines the effective size of eddies responsible for scattering. Thus a_1^2 varies with the different probing wavelengths. A relationship between spectral slope and C_n^2 shall enable appropriate C_n^2 be given for different turbulence conditions.

References

- 1 deWolf D A, *Radio Sci (USA)*, **10** (1975) 53.
- 2 Crane R K, *Paper presented at the fourteenth weather radar conference, American Meteorological Society, Boston, Massachusetts, USA, 1970.*
- 3 Ecklund W L, Carter D A & Gage K S, *J Geophys Res (USA)*, **82** (1977) 4969.
- 4 Chadwick R B, Moran K P, Morrison G E & Campbell W C, *Rep No. AFGL-TR-78-0160, Wave Propagation Laboratory, Boulder, Colorado, USA, 1978.*
- 5 Chadwick R B & Moran K P, *Radio Sci (USA)*, **15** (1980) 355.
- 6 Gossard E E, *Radio Sci (USA)*, **12** (1977) 89.
- 7 Mieghem J V, *Atmospheric Energetics* (Clarendon Press, Oxford) 1973.
- 8 Hufnagel R E, *Topical meeting on optical propagation through turbulence, Optical Society of America, Washington DC, USA, 1974, pp. Wal-1 to Wal-4.*
- 9 VanZandt T E, Green J L, Gage K S & Clark W L, *Radio Sci (USA)*, **13** (1978) 819.
- 10 Tatarskii V K, *The effects of the turbulent atmosphere on wave propagation* (National Technical Information Service, Springfield, USA), 1971.
- 11 Gjessing D T, Kjellass A G & Nordo J, *J Atmos Sci (USA)*, **26** (1969) 462.
- 12 Brook R R, *Boundary Layer Meteorol (Netherlands)*, **15** (1978) 481.
- 13 Reinking R F, *Boundary Layer Meteorol (Netherlands)*, **19** (1980) 373.
- 14 Ottersten H, *Radio Sci (USA)*, **4** (1969) 119.
- 15 Tatarskii V I, *Wave propagation in a turbulent medium* (McGraw-Hill Book Co. Inc., New York) 1961.
- 16 Pasricha P K, Sarkar S K, Banerjee P K & Ramakrishna M, *J Inst Electron & Telecomm Eng (India)*, **25** (1979) 240.